

# Frequency Estimation Algorithms by Fusion Spectra of Multi-section Sinusoids

**Abstract.** For achieving a more precise frequency estimation of a short sinusoid at low SNR, a algorithm based on fusion spectra of Multi-section Sinusoids(M-sinusoids) was proposed. In order to solve the discontinuous phases problem of M-sinusoids, the Optimization Weighted-Accumulation (OW-A) spectrum was gained through weighted-accumulation spectra of M-sinusoids by the designed weighted factor. The correlation spectrum, which could inherit the narrow and high main-lobe of the OW-A spectrum, and the good noise immunity of the accumulation spectrum of M-sinusoids, was constructed by correlation OW-A spectrum and the accumulation spectrum. Therefore, higher precision frequency estimation could be obtained through spectral peak searching of the correlation spectrum. Moreover, in order to meet the high real-time demand in some fields, a fast algorithm of the proposed algorithm was put forward. This fast algorithm could reduce most computational cost of the proposed algorithm by the following techniques: design a fast DTFT algorithm, reduction dimensions of the weighted fusion spectrum matrix, 1/3 main-lobes correlation of the OW-A spectrum and the accumulation spectrum. Simulations demonstrate the superior performance of the proposed algorithms; the fast algorithm could reduce most calculation of the proposed algorithm with lowering a little frequency estimation precision, and it works better in very low SNR (SNR≤-13dB).

**Streszczenie.** W artykule zaproponowano algorytm estymacji częstotliwości krótkich fal sinusoidalnych o niskim zaszumieniu (SNR). Rozwiązanie bazuje na widmie fuzji M-częstotliwości sinusoid (M-sinusoids). W celu rozwiązania problemu nieciągłości faz M-sinusoid zastosowano współczynniki wagowe zawartości częstotliwości, co pozwoliło na ich optymalizację (ang. Optimization Weighted-Accumulation). Zastosowanie algorytmu pozwala na zwiększenie precyzji estymacji przy jednoczesnym zwiększeniu szybkości wykonania. Wyniki badań symulacyjnych potwierdzają skuteczność działania. (Estymacja częstotliwości z wykorzystaniem widma fuzji M-częstotliwości sinusoid).

**Key Words:** Frequency estimation, Spectra fusion, Multi-section Sinusoids (M-sinusoids), Signal processing

**Słowa kluczowe:** estymacja częstotliwości, widmo fuzji, multi-częstotliwość sinusoid, przetwarzanie sygnału.

## 1. Introduction

Precise frequency estimation for the short sinusoid signal at low Signal-to-Noise Ratio(SNR) has a significant theoretical and practical value in many fields, such as radar, sonar communication, speech recognition, fault diagnosis and image processing[1]-[3]. Due to its short duration, the spectrum of a short sinusoid signal has a severe spectrum leakage, insufficient information and a poor anti-noise property [4], which effect the frequency estimation precise heavily. In order to solve those problems above perfectly, a frequency estimation algorithm based on fusion spectra of Multi-section Sinusoids (M-sinusoids) was proposed. This algorithm can accumulate information of M-sinusoids by fusion spectra of M-sinusoids. In opinion of information theory, information of M-sinusoids is several times than that of a single section sinusoid, therefore fusion spectra of M-sinusoids is an effective way to make up the insufficient information and severe spectrum leakage of a short section signal, which can improve frequency estimation precision largely from the signal source without heavy hardware cost[5]-[6]. Moreover, in order to meet the high real-time demand in some fields such as radar, sonar and electronic countermeasures, a fast algorithm of the proposed algorithm was also put forward. This fast algorithm could reduce most calculation of the proposed algorithm by the following techniques: design a fast DTFT algorithm, reduction dimensions of the weighted fusion spectrum matrix, correlation between the 1/3 main-lobes of the OW-A

spectrum and the accumulation spectrum.

This paper is organized as follows: section 2 describes the principle of the frequency estimation algorithm based on fusion spectra of M-sinusoids. A fast algorithm of the proposed algorithm is given in Section 3. Section 4 analyze the computation of the proposed algorithms. Section 5 gives the performance simulation of the proposed algorithms, including the frequency estimation algorithm and its fast algorithm. Section 6 gives the conclusions and the vision of future work.

## 2. Frequency estimation algorithm based on fusion spectra of M-sinusoids

The principle of the frequency estimation algorithm based on fusion spectra of M-sinusoids is shown in figure 1. Firstly, spectra of M-sinusoids are generated. In order to solve problems caused by the discontinuous phases and the serious spectrum leakage, the Optimization Weighted-Accumulation (OW-A) spectrum is gained through weighted-accumulation spectra of M-sinusoids by the designed weighted-factor. To restrain noise interference and the false spectral peaks, the correlation spectrum is constructed by correlation the OW-A spectrum and the accumulation spectrum of M-sinusoids. Finally, exact frequency estimation can be obtained through spectral peak searching of the correlation spectrum. The following part focuses on the generation of M-sinusoids' spectra, the OW-A spectrum and the correlation spectrum.

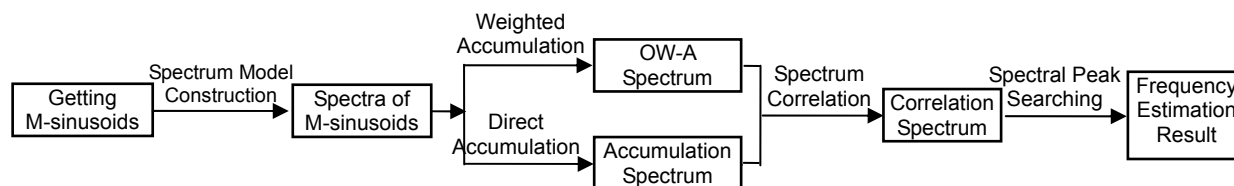


Fig.1. The principle of the frequency estimation algorithm based on fusion spectra of M-sinusoids

## 2.1. Spectra of M-sinusoids

$x$  Represents  $M$  ( $M \geq 2$ ) sections M-sinusoids,  $x_m$  ( $m \in [1, M]$ ) represents the  $m$  th section signal in  $x$ , (1)  
 $x_m(n_m) = \cos[\theta(m) + 2\pi n_m f / f_s]$ ,  $n_m \in [1, N_m]$

Where:  $f$  - the estimated frequency of  $x$ ,  $f_s$  - the sampling frequency,  $n_m$  - the sampling index,  $N_m$  - the sampling point  $\theta(m)$  - the initial phase of the  $m$  th section signal of  $x$

respectively. The sampling point of  $x$  is  $N = \sum_{m=1}^M N_m$ . Any  $\theta(m)$  and  $\theta(m+1)$  are often discontinuous, that is  $\theta(m+1) \neq \theta(m) + 2\pi N_m f / f_s$ .

Assuming  $f_{scope}$  is the approximate value range of  $f$ . Make  $f_{scope}$  linear divided, create a sequence  $f_P$  with the length of  $P$  ( $P \geq 2$ ) and a sequence  $f_Q$  with the length of  $Q$  ( $Q \geq 2$ ). Where  $f_P(p)$  denotes the  $P$  th element of  $f_P$ ,  $p \in [1, P]$ ;  $f_Q(q)$  denotes the  $q$  th element of  $f_Q$ ,  $q \in [1, Q]$ ;  $f_P(p_q)$  denotes the element which the most approximately equals to  $f_Q(q)$  in  $f_P$ , that is  $f_P(p_q) \approx f_Q(q)$ ,  $p_q \in [1, P]$ . As the spectrum of any real signal is conjugate symmetric, it is impossible to loss information and bring false information excluding the negative frequency part[3]. Therefore, the spectrum in the part of positive frequency is only considered in this paper.

Calculate Discrete Time Fourier Transform(DTFT) of  $x_m$  at  $f_P(p)$ , and record its positive part as  $X_m[f_P(p)]$ , record the one-dimensional vector composed of all  $X_m[f_P(p)]$  as  $X_m(f_P)$ .

$$(2) X_m[f_P(p)] = 0.5 \sum_{n_m=1}^{N_m} e^{j[\theta(m) + 2\pi n_m f / f_s]} e^{-j2\pi n_m f_P(p) / f_s} = \frac{\sin[N_m g(p)]}{2 \sin g(p)} e^{j[\theta(m) + g(p)(N_m + 1)]}$$

$$(3) X_m(f_P) = \{X_m[f_P(1)], \dots, X_m[f_P(P)]\}$$

where:  $g(p) = \pi[f - f_P(p)] / f_s$ .

$\theta_z(m, p)$  denotes the phase character of  $X_m[f_P(p)]$  in noises, calculated by equation (4),

$$(4) \theta_z(m, p) = \text{angle}\{X_m[f_P(p)] + W_m[f_P(p)]\}$$

where:  $\text{angle}(t)$  - a function of calculation the phase of plural  $t$ ,  $W_m[f_P(p)]$  - the influence of noises on  $X_m[f_P(p)]$ ,  $f_P(p_0)$  - an estimated value of  $f$ . Therefore,  $\theta_z(m, p_0)$  can approximately equal to  $\theta(m)$  when SNR is not very low, and  $\theta(m)$  can be replaced by  $\theta_z(m, p_0)$  in equation (3) in noises.

$s$  denotes a phase continuous sinusoidal signal with the same sampling point as  $x$ ,

$$(5) s(n_s) = \cos[\theta(1) + 2\pi n_s f / f_s]$$
,  $n_s \in [1, N]$

Divide  $s$  into  $M$  sections signals, whose sampling point is  $N_m$  ( $m \in [1, M]$ ) in turn. Calculate DTFT of  $s$  at  $f_P(p)$ , record its positive part as  $S[f_P(p)]$ , record the one-dimensional vector composed of all  $S[f_P(p)]$  as  $S(f_P)$ , and regard  $S(f_P)$  as the spectrum of  $s$ .

$$(6) S[f_P(p)] = \sum_{m=1}^M \sum_{n_m=1}^{N_m} 0.5 e^{j[\theta(1) + 2\pi g(p)(\sum_{m=1}^m N_m - N_m + n_m)]}$$

$$(7) = \sum_{m=1}^M \frac{\sin[N_m g(p)]}{2 \sin g(p)} e^{j[\theta(1) + g(p)(2 \sum_{m=1}^m N_m - N_m + 1)]}$$

$$S(f_P) = \{S[f_P(1)], \dots, S[f_P(P)]\}$$

## 2.2. OW-A Spectrum

Due to the short duration of  $x_m$ , the main-lobe of  $X_m(f_P)$  is wide and its anti-noise is poor. In order to solve these problems, a weighted-factor  $e^{-jD}$  is designed to fuse  $M$  sections  $X_m(f_P)$  to the OW-A Spectrum, which is approximately as same as the spectrum of a phase-continuous sinusoid with the same length of  $x$ .  $e^{-jD(m, p, q)}$  denotes the  $(m, p, q)$  th element in  $e^{-jD}$ .

$$(8) e^{-jD(m, p, q)} = e^{-j[\theta_z(m, p_q) - \theta_z(1, p_q) - 2g_q(p)(\sum_{m=1}^m N_m - N_m)]}$$

Where:  $g_q(p) = \pi[f_Q(q) - f_P(p)] / f_s$ .

$X'(f_P)$ , which is gained by weighted accumulation of  $X_m(f_P)$  with  $e^{-jD}$ , represents the weighted-accumulation spectrum matrix of  $x$ .  $X_q'(f_P)$  denotes the elements in the  $q$  th column of  $X'(f_P)$ ,  $X_q'[f_P(p)]$  denotes the  $(p, q)$  th element in  $X'(f_P)$ . Searching  $\text{MAX}\{abs[X'(f_P)]\}$ , the column in which the peak element located is  $q_0$ , and all elements in the  $q_0$  th column of  $X'(f_P)$  compose  $X_{q_0}'(f_P)$ . As shown in figure 2,  $X_{q_0}'(f_P)$  is similar to the spectrum  $S(f_P)$  of the phase-continuous signal  $s$ . The main-lobe of  $X_{q_0}'(f_P)$  is narrow and high, the energy of  $X_{q_0}'(f_P)$  is relatively concentrated, the spectrum leakage is weakened obviously, so  $X_{q_0}'(f_P)$  is regarded as the OW-A spectrum.

$$(9) X_q'[f_P(p)] = \sum_{m=1}^M \{e^{-jD(m, p, q)} X_m[f_P(p)]\}$$

$$(10) X_q'(f_P) = \{X_q'[f_P(1)], \dots, X_q'[f_P(P)]\}$$

$$(11) X'(f_P) = [X_1'(f_P), \dots, X_Q'(f_P)]$$

$$= \left\{ \begin{array}{l} X_1'[f_P(1)], \dots, X_Q'[f_P(1)] \\ \dots \\ X_1'[f_P(P)], \dots, X_Q'[f_P(P)] \end{array} \right\}$$

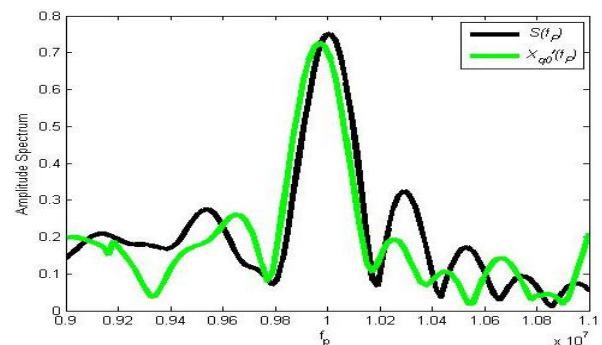


Fig. 2. Amplitude Spectrum of  $S(f_P)$  and  $X_{q_0}'(f_P)$

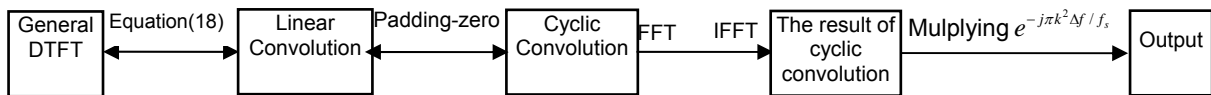


Fig.3. The basic idea of the proposed fast DTFT algorithm.

### 2.3. Correlation Spectrum

Frequency-domain correlation performs as the accumulation of the product of co-frequency components[5]. Take advantage of the frequency of a sinusoid locates around the spectrum peak, spectrum correlation technology in this paper is mainly used to analyze the correlation of two different types spectrum of the same signal, that is the OW-A spectrum and the accumulation spectrum. It can reduce noises and improve signal parameters estimation precision.

$X(f_p)$  calculated as equation(12), represents the accumulation spectrum of  $X_m(f_p)$ ,

$$(12) \quad X(f_p) = \sum_{m=1}^M abs[X_m(f_p)]$$

As the accumulation spectrum  $X(f_p)$  can increase the main lobe's height and reduce noises to some extent[6], the main-lobe of  $X_{q_0}'(f_p)$  is narrow and high, the energy of  $X_{q_0}'(f_p)$  is relatively concentrated, the spectrum leakage is weakened obviously. Make correlation analysis for  $X_{q_0}'(f_p)$  and  $X(f_p)$ , which can combine good characters of the narrow high main-lobe of  $X_{q_0}'(f_p)$  and the good anti-noise of  $X(f_p)$ .

Calculate the correlation spectrum  $r(f_p)$  of  $X_{q_0}'(f_p)$  and  $X(f_p)$  as equation (13) and (14),

$$(13) \quad r[f_p(p)] = \{X[f_p(p)] + W[f_p(p)]\} \times \{X_{q_0}'[f_p(p)] + W_{q_0}[f_p(p)]\} \\ = X[f_p(p)]W_{q_0}[f_p(p)] + X_{q_0}'[f_p(p)]W[f_p(p)] \\ + W_{q_0}[f_p(p)]W[f_p(p)] + X[f_p(p)]X_{q_0}'[f_p(p)]$$

$$(14) \quad r(f_p) = \{r[f_p(1)], \dots, r[f_p(P)]\}$$

where:  $W(f_p)$ -the noises on  $X(f_p)$ ,  $W_{q_0}(f_p)$ -the noises on  $X_{q_0}'(f_p)$ . As the randomness of noises, it is generally thought that there are little correlation between  $X(f_p)$  and  $W_{q_0}(f_p)$ , between  $X_{q_0}'(f_p)$  and  $W(f_p)$ . Due to the weighted factor, the correlation of  $W_{q_0}(f_p)$  and  $W(f_p)$  is weak compared to that of  $X(f_p)$  and  $X_{q_0}'(f_p)$ . Therefore, equation (14) mainly considers the correlation of  $X(f_p)$  and  $X_{q_0}'(f_p)$  without noises. Moreover, it is easy to reduce noises through calculation the correlation spectrum  $r(f_p)$ , as  $X(f_p)$  and  $X_{q_0}'(f_p)$  are generated from the same signal  $x$ ,  $X(f_p)$  and  $X_{q_0}'(f_p)$  can get the peak at the same frequency point, which is closest to the true frequency  $f$  without noises interference. At that time, the correlation of  $X(f_p)$  and  $X_{q_0}'(f_p)$  is strongest, so spectrum peak of  $r(f_p)$  can get the optimal estimation of  $f$ .

### 3. Fast algorithm of the proposed algorithm

The calculation of the proposed algorithm based on fusion spectra of M-sinusoids (called it the pre-proposed algorithm for short) mainly focuses on the following three parts: calculation  $X_m(f_p)$  through DTFT, generation the OW-A Spectrum  $X_{q_0}'(f_p)$  and calculation the correlation spectrum  $r(f_p)$ . In order to meet the high real-time demand in some fields such as radar, sonar and electronic countermeasures, a fast algorithm for the proposed algorithm was proposed. The fast algorithm can reduce most calculation with lower little precision by some techniques as follow: design a fast DTFT algorithm, reduction dimensions of the weighted fusion spectrum matrix, analyse the 1/3 main-lobes correlation of the OW-A spectrum and the accumulation spectrum.

#### 3.1. The fast DTFT algorithm

##### 3.1.1. Principle of the fast DTFT algorithm

According to the above analyse, the calculation cost of  $X_m(f_p)$  through DTFT in the pre-proposed algorithm is heavy. Though paper[7] has proposed a fast DTFT algorithm, it can not deal with the sequence with the fix length in the pre-proposed algorithm.

The general definition of DTFT of a sequence  $x(n)$  is defined as equation (15)[3],

$$(15) \quad X(e^{j\Omega T_s}) = \sum_{n=0}^{N-1} x(n)e^{-j\Omega T_s n}$$

Take  $f_{scope} = [f_{min}, f_{max}]$ , the frequency resolution  $\Delta f$  and  $f_s$  into equation(15). An  $K$ -point DTFT is given by equation (16), where:  $K = (f_{max} - f_{min}) / \Delta f + 1$ .

$$(16) \quad X(e^{j\Omega T_s}) = \sum_{n=0}^{N-1} x(n)e^{-j\Omega T_s n} \\ = \sum_{n=0}^{N-1} x(n)e^{-jn(2\pi f_{min}/f_s + 2\pi \Delta f k / f_s)}, \quad k = 0, 1, \dots, K-1$$

Design a fast DTFT algorithm according to equation(17) proposed by Bluestein[8]

$$(17) \quad ab = \frac{1}{2}[a^2 + b^2 - (a-b)^2]$$

Equation(16) can be rewrite as equation(18):

$$(18) \quad X(e^{j\Omega T_s}) = e^{-j\pi k^2 \Delta f / f_s} \sum_{n=0}^{N-1} g(n)h(k-n)$$

where:

$$(19) \quad g(n) = x(n)e^{-j2\pi n(f_{min} + 0.5n\Delta f)/f_s}, \quad n = 0, 1, \dots, N-1$$

$$(20) \quad h(n) = e^{j\pi n^2 \Delta f / f_s}$$

According to equation(18)-(20),  $K$ -point DTFT of  $x(n)$  can be gotten by  $e^{-j\pi k^2 \Delta f / f_s}$  multiplying the linear convolution of  $g(n)$  and  $h(n)$  in fact. In order to compute the linear convolution of  $g(n)$  and  $h(n)$ , it only needs to choose the value of  $h(n)$  in the range  $-N+1 \leq n \leq K-1$ . So  $h(n)$  can be seen as a sequence with the length  $L = K + N - 1$ .

Calculation linear convolution in time-domain is inefficient, and results of cyclic convolution and linear convolution are the same when the length of cyclic convolution is greater than or equal to  $L + N - 1$ . Therefore, linear convolution of  $g(n)$  and  $h(n)$  can be convert into cyclic convolution with the cycle length  $L$ .

The proposed fast DTFT algorithm is described as figure 3, implementation steps are as follow:

Step 1: choose  $L$ .  $L$  is the smallest integer greater than or equal to  $K + N - 1$ , and the integer power of two.

Step 2: convert  $h(n)$  into a new sequence  $h_L(n)$  according to equation(21).

$$(21) \quad h_L(n) = \begin{cases} h(n), & 0 \leq n \leq K-1 \\ 0, & K \leq n \leq L-N \\ h(L-n), & L-N+1 < n < L-1 \end{cases}$$

Step 3: compute  $g(n)$  according to equation (19).

Step 4: convert  $g(n)$  into a new sequence  $g_1(n)$  by

padding-zero. Calculation  $L$ -point DFT of  $g_1(n)$  by the FFT and record its result  $G(l)$ .

Step 5: compute  $L$ -point DFT of  $h_L(n)$  by the FFT and record its result as  $H(l)$ .

Step 6: multiply  $G(l)$  and  $H(l)$  point by point and record the result as  $Y(l)$ , which is the cyclic convolution of  $g(n)$  and  $h(n)$ . Calculation  $L$ -point Inverse Fast Fourier Transform (IFFT) of  $Y(l)$ , and record its result as  $y'(n)$ . Record the value of  $y'(n)$  in the range of  $0 \leq n \leq K-1$  as  $y''(n)$ , which is the result of the linear convolution of  $g(n)$  and  $h(n)$ .

Step 7: multiply  $y''(n)$  by  $e^{-j\pi k^2 \Delta f / f_s}$  to give  $K$ -point DTFT of  $x(n)$ .

### 3.1.2. Computation analysis of the fast DTFT algorithm

(1) Calculation  $g(n)$ : needs  $N$  complex multiplications;

(2) Three times to calculate  $L$ -point FFT(step4,step5 and step6): needs  $1.5L \log_2 L$  complex multiplications and  $3L \log_2 L$  complex addition;

(3) Calculation the cyclic convolution of  $g(n)$  and  $h(n)$ : needs  $L$  complex multiplications;

(4) Calculation the multiplication of  $y''(n)$  and  $e^{-j\pi k^2 \Delta f / f_s}$ : needs  $K$  complex multiplications;

According to the above analysis, calculation  $K$ -point DTFT by the proposed fast algorithm needs about  $S'_{DTFT \times}$  complex multiplications and  $S'_{DTFT+}$  complex additions. Calculation  $K$ -point DTFT by the general DTFT algorithm needs about  $S_{DTFT \times} = KN$  complex multiplications and  $S_{DTFT+} = (N-1)K$  complex additions.

$$(22) \quad S'_{DTFT \times} = 1.5L \log_2 L + N + L + K$$

$$(23) \quad S'_{DTFT+} = 3L \log_2 L$$

### 3.2. Reduction dimensions of weighted fusion Spectrum matrix

$X'(f_p)$ , the weighted-accumulation spectrum matrix of  $x$ , is gotten through fusion all  $X_m(f_p)$  by the

weighted-factor  $e^{-jD}$ .  $X_m(f_p)$  is a  $P \times 1$  order matrix,  $e^{-jD}$  is a  $M \times P \times Q$  order matrix, so  $X'(f_p)$  is a  $P \times Q$  matrix, which can be described as figure 4. Figure 4 is a grid which is composed of  $P$  transverse lines and  $Q$  vertical lines. The intersection of the  $p$ th transverse line and the  $q$ th vertical line represents  $X'_q[f_p(p)]$ , which is the  $(p, q)$  the element in  $X'(f_p)$ .  $X_{q_0}(f_p)$  Can be represented by all elements on the  $q_0$ th vertical line.

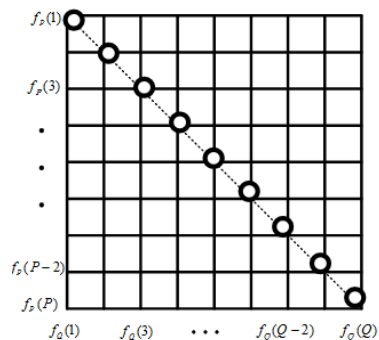


Fig.4. The principle diagram of the dimension reduction for weighted-fusion spectrum matrix

(1)  $P \neq Q$ .  $X_{q_0}(f_p)$  May locate on any column of  $X'(f_p)$ . So  $X_{q_0}(f_p)$  is confirmed only to spectrum peak search  $abs[X_{q_0}(f_p)]$  without noises. In that case, it is necessary to calculate all elements of  $X'(f_p)$ , which computational cost is heavy.

(2)  $P \neq Q$ .  $\square$  In the case of  $f = f_p(p_1)$  ( $p_1 \in [1, P]$ ), the peak of  $abs[X_{q_0}(f_p)]$  must locate at the  $(p_1, q_1)$ th of  $X'(f_p)$ , where  $p_1 = q_1$ . That is the peak of  $abs[X_{q_0}(f_p)]$  located at the diagonal of  $X'(f_p)$ . In the case of  $f \approx f_p(p_1)$ , the peak of  $abs[X_{q_0}(f_p)]$  must locate at the  $(p_1, q_1)$ th of  $X'(f_p)$ , where  $p_1 = q_1$ . The peak of  $abs[X_{q_0}(f_p)]$  located at the diagonal of  $X'(f_p)$ , too. Therefore, the peak of  $abs[X_{q_0}(f_p)]$  must locate at the diagonal of  $X'(f_p)$  when  $P = Q$ . In order to confirm  $X_{q_0}(f_p)$ , it is only necessary to calculate the elements at the diagonal of  $X'(f_p)$ . Let  $X_{pq}(f_p)$ , which is a  $P \times 1$  order matrix, represent all elements at the diagonal of  $X'(f_p)$ .  $X_{q_0}(f_p)$  can be confirmed through spectrum peak searching  $abs[X_{pq}(f_p)]$ . So it converts calculation a  $P \times Q$  order matrix  $X'(f_p)$  into calculation a  $P \times 1$  order matrix  $X_{pq}(f_p)$ , which can reduce the computational complexity.

$$(24) \quad X_{pq}(f_p) = \{X_1[f_p(1)], \dots, X_Q[f_p(Q)]\}$$

Moreover, reduction dimensions of the weighted fusion spectrum matrix are good for improving the anti-noise property. According to the analyse,  $X_{q_0}(f_p)$  should locate at the diagonal of  $X'(f_p)$  when  $P = Q$ . However,  $X_{q_0}(f_p)$  may be not found on the diagonal of  $X'(f_p)$

through spectrum peak searching  $abs[X_q'(f_P)]$  when  $P=Q$  in noises. While reduction dimensions of the weighted fusion spectrum matrix can confirm  $X_{q_0}'(f_P)$  located at the diagonal of  $X'(f_P)$ , which can improving the anti-noise property of the fast algorithm.

### 3.3. Correlation of the 1/3 main-lobes

Correlation analysis for  $X_{q_0}'(f_P)$  and  $X(f_P)$  can combine good characters of the narrow and high main-lobe of  $X_{q_0}'(f_P)$ , and the good anti-noise of  $X(f_P)$ , which can improve the spectrum analysis precision enormously. However, the 1/3 main-lobe of  $X_{q_0}'(f_P)$  has the biggest correlation with the same part of  $X(f_P)$ , so it is not necessary to analyse the correlation of  $X_{q_0}'(f_P)$  and  $X_{q_0}'(f_P)$  in the whole  $f_{scope}$ , only in the 1/3 main-lobe part, which is shown in gray part of figure 5. In that case, analyse the correlation of the 1/3 main-lobes can also decrease the calculation.

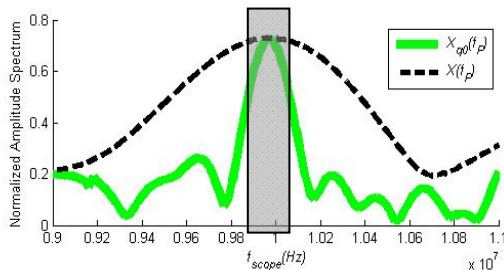


Fig. 5. The schematic diagram of correlation of the 1/3 main-lobe

Compute the correlation the 1/3 main-lobes spectrum  $r_{1/3}(f_P)$  of  $X_{q_0}'(f_P)$  and  $X(f_P)$  as equations (25,26)

$$(25) \quad r_{1/3}[f_P(pp)] = \{X[f_P(pp)] + Z[f_P(pp)]\}$$

$$\times \{X_{q_0}'[f_P(pp)] + Z_{q_0}[f_P(pp)]\}$$

$$\approx X[f_P(pp)] \times X_q'[f_P(pp)]$$

$$(26) \quad r_{1/3}(f_P) = \{r_{1/3}[f_P(pp)], \dots, r_{1/3}[f_P(pp)]\}$$

where:  $pp = p_{l_1}, p_{l_1} + 1, \dots, p_{l_2} - 1, p_{l_2}$

$$P_{l_1 l_2} = abs(p_{l_2} - p_{l_1}) < P, p_{l_1} \in [1, P], p_{l_2} \in [1, P],$$

$p_{l_2} \geq p_{l_1}, f_P(p_{l_1})$  - the  $p_{l_1}$  th element in  $f_P, f_P(p_{l_2})$  - the  $p_{l_2}$  th element in  $f_P$ , which are the discrete frequency points of the left and right respectively of the 1/3 main-lobe of  $X_{q_0}'(f_P)$ .

### 4. Computation analysis of the proposed algorithms

The computation of the pre-proposed algorithm, the fast algorithm (called them the proposed algorithms for short) is shown in table 1 and table 2 respectively. As the complex operation is the main operation of the proposed algorithms in the paper, the complex multiplication and complex addition are choose as the compared criterion.

Convert the complex operation into the real operation according to the follow relationships: one complex multiplication equates to four real multiplications and two real additions, one complex addition equates to two real additions. Set  $M=4, P=150, Q=150, N_m=50, N=200, L_m=256, (m \in [1, M])$ ,  $P_{l_1 l_2} = P/5$ , and take TMS320VC5502[9] as the processor with the main frequency 100MHz (which the max main frequency is 300 MHz). According to the following criterion: calculating one real multiplication needs two instruction cycles, one real addition needs one instruction cycle, the time consuming of the proposed algorithms are shown in table 3. Moreover, the time consuming of the proposed fast algorithm can decrease more with the increasing of the main frequency of TMS320VC5502.

Table 1. Computation of the pre-proposed algorithm

	The pre-proposed algorithm	
	Times of complex multiplication	Times of complex addition
Compute $M X_m(f_P)$	$N \times P$	$(N - M) \times P$
Compute $X'(f_P)$	$P \times Q \times M$	$(M - 1) \times P \times Q$
Compute $X(f_P)$	0	$M - 1$
Compute $r(f_P)$	$P$	0
Sum	$P(QM + N + 1)$	$(M - 1)(PQ + 1) + P(N - M)$

Table 2. Computation of the fast algorithm

	The fast algorithm	
	Times of complex multiplication	Times of complex addition
Compute $M X_m(f_P)$	$\sum_{m=1}^M (1.5L_m \log_2 L_m + N_m + L_m + P)$	$\sum_{m=1}^M 3L_m \log_2 L_m$
Compute $X_{pq}'(f_P)$	$M \times P$	$(M - 1) \times P$
Compute $X_{q_0}'(f_P)$	$M \times P$	$(M - 1) \times P$
Compute $X[f_P(pp)]$	0	$M - 1$
Compute $r_{1/3}(f_P)$	$P_{l_1 l_2}$	0
Sum	$\sum_{m=1}^M (1.5L_m \log_2 L_m + L_m) + 3MP + N' + P_{l_1 l_2}$	$\sum_{m=1}^M 3L_m \log_2 L_m + (M - 1)(2P + 1)$

Table 3. Computation and time consuming of the proposed algorithms

Computation	The pre-proposed algorithm	The fast algorithm
Times of complex addition	96903	25479
Time consuming of complex addition(ms)	1.9381	0.5096
Times of complex multiplication	120150	15342
Time consuming of complex multiplication(ms)	12.0150	1.5342
Sum(ms)	13.9531	2.0438

**5. Simulation validation**

To validate the proposed algorithms, compared experiments with the algorithm in paper[10] and FFT+FT[11] are implemented in Matlab7.9. The frequency estimation object of the proposed algorithms and FFT+FT are  $b_1$  and  $b_2$ , which denote  $M$  sections M-sinusoids with equal length and M-sinusoids with unequal length respectively.  $N_{1m}(m)$  and  $N_{2m}(m)$  denote the sampling point of the

$m$  th section signal of  $b_1$  and  $b_2$  respectively. The algorithm in paper[10] only fits  $M$  sections M-sinusoids with equal length, so its frequency estimation object is  $b_1$ .  $f_{scope}$  can be gained from the FFT. The noise added in the experiments is additive Gaussian white noise. Experiment parameters are shown in table 4.

Table 4. Experiment Parameters

Parameters	SNR	$f$	$f_s$	$M$	$[N_{11}, \dots, N_{1M}]$	$[N_{21}, \dots, N_{2M}]$	$P$	$Q$
Setting	-5dB	10MHz	40MHz	4	[50, 50, 50, 50]	[15, 20, 100, 105]	150	150

Table 5. RMSE of frequency estimation in different SNR

SNR (dB)	The pre-proposed algorithm RMSE(KHz)		The fast algorithm RMSE(KHz)		The algorithm in [10] RMSE(KHz)		FFT+FT RMSE(KHz)	
	$b_1$	$b_2$	$b_1$	$b_2$	$b_1$	$b_2$	$b_1$	$b_2$
-15	149.61	146.75	145.48	143.30	218.45		398.98	369.55
-13	84.18	77.86	81.30	71.74	138.74		349.24	318.92
-11	51.39	43.46	57.25	48.21	127.87		286.16	243.15
-9	42.57	39.21	46.42	43.80	120.08		238.63	156.67
-7	41.27	36.56	43.02	40.57	104.59		212.20	122.79
-5	38.02	35.80	39.61	37.87	96.73		208.16	108.89
-3	35.66	34.08	37.25	35.28	90.74		195.25	102.95
-1	33.16	32.32	35.34	34.29	82.16		192.82	96.02
1	32.85	31.33	33.87	31.46	76.36		192.62	97.81
3	30.49	29.07	32.05	30.04	77.42		192.21	96.37

**5.1. Comparison Experiments at Low SNR**

To test the performance of the pre-proposed algorithm, the fast algorithm, the algorithm in paper[10] and FFT+FT at low SNR, 1000 times Monte-Carlo experiments are carried out at SNR=-5dB. Other experiment parameters are shown in table 4.

(1) For estimation the frequency of signal  $b_1$ , Root Mean Square Errors (RMSE) of the four methods mentioned above are [38.02, 39.61, 96.39, 212.20]KHz respectively. RMSE of the fast algorithm is a little bigger than the pre-proposed algorithm, the error of the proposed algorithms is about 1/3 and 1/5 as that of the algorithm in paper[10] and FFT+FT respectively;

(2) For estimation the frequency of signal  $b_2$ , RMSE of the pre-proposed algorithm, the fast algorithm and FFT+FT is [35.80, 37.87, 108.89]KHz respectively. RMSE of the fast algorithm is very near to pre-proposed algorithm, the error of the proposed algorithms is about 1/3 as that of FFT+FT.

**5.2. Comparison experiments of different SNR**

To test the performance of the four methods mentioned above under the condition of different SNR, 11 groups experiments are made. Each group includes 1000 times Monte-Carlo experiments. Other experiment parameters are shown in table 4. Experiment results given in table 5 demonstrate that:

(1) RMSE of the four methods mentioned above decline along with the raise of SNR.

(2) The proposed algorithms have more super performance than other two methods for estimation the frequency of signal  $b_1$  and  $b_2$ .

(3) RMSE of the fast algorithm is very near to

pre-proposed algorithm.

**5.3. Comparison experiments of different length of one section signal**

To test the performance of the four methods mentioned above under the condition of different length of one section signal, 10 groups experiments are made. Each group includes 1000 times Monte-Carlo experiments. The length of one section signal in  $b_1$  and  $b_2$  is shown in table 6. Other parameters are shown in table 4. Experimental results shown in table 7 demonstrate that:

(1) RMSE of the four methods decline along with the raise of the length of one section signal in  $b_1$  and  $b_2$ .

(2) The proposed algorithms have more super performance than other two methods mentioned above for estimation the frequency of signal  $b_1$  and  $b_2$ .

(3) RMSE of the fast algorithm is very near to pre-proposed algorithm.

Table 6. The length of one section signal in  $b_1$  and  $b_2$

Group	$N_{b_1,1}, N_{b_1,2}, N_{b_1,3}, N_{b_1,4}$	$N_{b_2,1}, N_{b_2,2}, N_{b_2,3}, N_{b_2,4}$
1	50, 50, 50, 50	5, 10, 90, 95
2	55, 55, 55, 55	10, 15, 95, 100
3	60, 60, 60, 60	15, 20, 100, 105
4	65, 65, 65, 65	20, 25, 105, 110
5	70, 70, 70, 70	25, 30, 110, 115
6	75, 75, 75, 75	30, 35, 115, 120
7	80, 80, 80, 80	35, 40, 120, 125
8	85, 85, 85, 85	40, 45, 125, 130
9	90, 90, 90, 90	45, 50, 130, 135
10	95, 95, 95, 95	50, 55, 135, 140

Table 7. RMSE of frequency estimation in different length of one section signal in  $b_1$  and  $b_2$

Group	The pre-proposed algorithm RMSE(KHz)		The fast algorithm RMSE(KHz)		The algorithm in [10] RMSE(KHz)		FFT+FT RMSE(KHz)	
	$b_1$	$b_2$	$b_1$	$b_2$	$b_1$	$b_2$	$b_1$	$b_2$
1	38.02	35.80	39.61	37.87	96.730		204.27	105.34
2	34.17	35.33	35.37	35.04	86.189		184.39	103.12
3	34.05	34.27	34.67	35.00	81.095		166.87	100.47
4	32.80	33.95	33.12	34.41	73.476		152.99	93.71
5	32.04	33.87	32.78	34.02	73.580		144.07	89.57
6	31.34	33.41	32.67	33.93	68.534		133.71	89.22
7	31.04	33.22	31.70	33.46	64.633		118.75	85.90
8	29.97	32.67	31.40	33.10	61.781		117.38	84.51
9	29.82	32.52	30.93	32.93	60.446		107.24	81.65
10	29.67	31.48	30.24	32.74	57.661		102.13	78.68

**5.4. Comparison experiments of different  $f$**

To test the performance of the four methods mentioned above under the condition of different  $f$ . 10 groups experiments are made. Each group includes 1000 times Monte-Carlo experiments. Other experiment parameters are shown in Table 4. Experiment results given in table 8 demonstrate that:

(1) The proposed algorithms have more super performance than other two methods mentioned above for estimation the frequency of  $b_1$  and  $b_2$ .

(2) RMSE of the fast algorithm is very near to pre-proposed algorithm.

Table 8. RMSE of frequency estimation in different  $f$

$f_0$ (MHz)	The pre-proposed algorithm RMSE(KHz)		The fast algorithm RMSE(KHz)		The algorithm in [10] RMSE(KHz)		FFT+FT RMSE(KHz)	
	$b_1$	$b_2$	$b_1$	$b_2$	$b_1$	$b_2$	$b_1$	$b_2$
7.5	37.36	36.13	38.75	36.52	96.161		199.00	158.66
8.0	37.38	36.12	38.45	36.53	95.274		202.73	105.20
8.5	38.01	36.10	38.30	37.15	96.147		218.29	104.74
9.0	36.76	36.13	37.36	36.50	91.623		215.43	107.64
9.5	38.16	36.61	38.35	37.93	98.278		198.12	103.94
10.0	38.02	35.80	39.61	37.87	97.513		198.55	100.55
10.5	37.80	36.25	38.69	37.91	93.224		194.31	99.49
11.0	35.50	36.38	36.88	38.31	91.399		215.71	108.96
11.5	37.02	36.13	37.47	37.66	92.730		201.61	107.00
12.0	38.13	36.55	38.84	37.11	98.488		201.90	100.04
<b>Mean(KHz)</b>	37.41	36.22	38.27	37.35	95.084		204.56	109.62

**6. Conclusions and future work**

A frequency estimation algorithm based on spectra correlation of M-sinusoids was proposed. To solve the problems caused by the discontinuous phases and serious spectrum leakage of M-sinusoids, the OW-A spectrum is gained through weighted-accumulating spectra of M-sinusoids by the designed weighted factor. To reduce the interference of noises, inherit the narrow and high main lobe of the OW-A spectrum and the good anti-noise feature of the accumulation spectra, the correlation spectrum is constructed by correlation the OW-A spectrum and the accumulation spectrum of M-sinusoids. Consequently, precise frequency estimation was obtained through spectral peak searching of the correlation spectrum. Moreover, a fast algorithm of the proposed algorithm was put forward to meet the high real-time demand in some fields. This fast algorithm could reduce most calculation of the above proposed algorithm by the following techniques: design a fast DTFT algorithm, reduction dimensions of the weighted fusion spectrum matrix, correlation between the 1/3 main-lobes of the OW-A spectrum and the accumulation spectrum. Calculation analyses and simulations demonstrate that the fast algorithm could reduce most calculation of the pre-proposed algorithm with lowering a little precision, and it works better in very low SNR(SNR≤-13dB). Simulation results demonstrate that the proposed algorithms have more superior performance compared with the algorithm in paper[10] and FFT+FT. In the low SNR=-5dB, RMSE of the proposed algorithm is about 1/3 and 1/5 as the same as that of the algorithm in paper[10] and FFT+FT for estimation the

frequency of  $b_1$ ; RMSE of the proposed algorithm is about 1/3 as the same as that of FFT+FT for estimation the frequency of  $b_2$ .

The future work of this paper is to make field experiments to validate the proposed algorithms, especially in some industrial environment.

**Acknowledgment**

The work is partially supported by Natural Science Foundation of China (Grant No. 61271449, No. 61201450, No.60871098) and Natural Science Foundation of Chongqing, China Grant No.cstc 2011BA2015, csct2012jjA0877, csct2012jjA1047).

**REFERENCES**

- [1] Geroleo F G., Brandt-Pearce M., Detection and estimation of LFM CW radar signals, *IEEE Transactions on Aerospace and Electronic Systems*, 48(2012), No.1,405-418.
- [2] Candan C., A method for fine resolution frequency estimation from three DFT samples. *IEEE SPL*,18(2011), No.6, 351-354.
- [3] Chan F., So H. C., Lau W. H., Chan C. F., Efficient approach for sinusoidal frequency estimation of gapped data, *IEEE Signal Processing Letters*, 17(2010), No.6, 611-614.
- [4] Prioakis J. G., Manolakis D. G., Digital signal processing: principle, algorithms, and application, *New Jersey: Prentice Hall*, 2006:112-114.
- [5] Gan S. M., Guo X. Z., Zhao Y. J., The signal correlation analysis, *Instrument Consumers*, 15(2008), No.4, 120-121.
- [6] Ju P. H., Qin S. R., Qin Y., Ding Z. Y., Research on earlier fault diagnosis of gear by method of multi-resolution empirical mode decomposition and frequency domain averaging.

- [7] *Journal of Vibration and Shock*, 28(2009), No.5, 97-101.
- [8] Zhang H. T., Tu Y. Q., New signal processing method with negative frequency contribution for Coriolismass flowmeter, *Chinese Journal of Scientific Instrument*, 28(2007), No.3, 539-544.
- [9] Bluestein L. I., A linear filtering approach to the computation of the discrete Fourier transform, *IEEE Transactions on Audio and Electroacoustics*, 18(1970), No.4, 451-455.
- [10] Zhao X. Q., Guo Y. C., DSP implementation and blind equalization algorithms based on coordinate transformation, *2010 2nd International Asia Conference on Informatics in Control, Automation and Robotics*, Wuhan, China, March 6 - 7, (2010), 79-82.
- [11] Liu L. B., Tu Y. Q., Zhang H. T., Fusion algorithm for frequency estimation of multi-section signals with same frequency and length, *Journal of System Simulation*, 21(2009), No.1, 194-198.
- [12] Ding K., Zhu W. Y., Yang Z. J., Li W. H., Parameter estimation accuracy of FFT and FT discrete spectrum correction, *Journal of Mechanical Engineering*, 46(2010), No.7, 48-73.

**Authors:** Wei Xiao, Yaqing Tu, Liangbing Liu and Yanlin Shen are with the Department of Logistical Information Engineering, Logistical Engineering University, Chongqing, China. Lei Zhang is with the Zhuozhou Comprehensive Storehouse, Hebei, China. Email: wzwry@163.com; yqtqc@sina.com; liuliangbing1981@sina.com; shenyalin@sina.com; zhanqlei@sina.com.